Available online at www.humg.edu.vn

ESASGD 2016

GIS-IDEAS (2016)

Conference Title: International Conference on GeoInformatics for Spatial-Infrastructure Development in Earth & Allied Sciences (GIS-IDEAS)

A comparison of fusion methods for SAR and Optical Imagery

Cao Xuan Cuong[a,]*, Nguyen Van Trung[a]

[a] *University of Mining and Geology, 18 Vien St, Duc Thang Ward, Bac Tu Liem District, Hanoi City 1000000, Vietnam*

Abstract

Multi-sensor image fusion, known as the process of combining the information acquired from different image sensors is to get a more comprehensive interpretation of scene. It is worthily noted that full integration of the images might lead to the unwanted result. Wavelet, the Intensity-Hue-Saturation (IHS), and the principle component analysis (PCA) methods have been commonly applied in the field of image fusion. This article presents two hybrid image fusion methods, namely PCA-Wavelet and IHS-Wavelet, with several injection models to merge the synthetic aperture radar (SAR) and optical images. The spectral distortion of fused results due to heterogeneous characteristic and speckle in SAR data was eliminated through selective fusion rules. The methods were applied to merge Landsat 5 TM data with the European Remote Sensing satellite-2 (ERS-2), the Phased Array Type L-band Synthetic Aperture Radar (ALOSPALSAR) data. Besides, weighted combination and full integration models were employed for fusing Landsat 8 OLI and Sentinel-1 data using PCA-Wavelet method. The results showed that PCA-wavelet performed better than IHS-wavelet and the full integration model was the best choice for the model of injection in PCA-wavelet method.

Keywords: Wavelet, IHS, PCA, fusion, SAR, optical data

---

1. Introduction

Image fusion has been increasingly common in the community of remote sensing because of the rapid development in sensor technologies. With more images from different sensors, the demand of producing optimally multi-sensor fused data for further applications such as change detection, object identification, and segmentation, has been increased and attracted numerous researchers. In the process of multisource image fusion, one focuses on combining information from different images to get a single image which achieves the advantages of input images. Then the fused results become more useful than any individual original image (Pohl & Van Genderen, 1998).

There have been a large number of publications describing various techniques for the integration of the synthetic aperture radar (SAR) and optical imagery (Alparone et al., 2004; Amarsaikhan et al., 2012; Byun, Choi et al., 2013; Hong & Mercer, 2009). As being well-known for all weather and day-night sensing system, the SAR imagery contains information which is decided by the characteristics of the surface target such as roughness, moisture, as well as the frequency of the illuminating electromagnetic radiation. This is different to the optical imagery as its information depends on the multispectral reflectance of the target illuminated by sunlight (Alparone et al., 2004). The integration of SAR and optical image is to get the better understanding of the objects observed within the imaged scene.

The loss and distortion of information as an inevitable consequence of image fusion might have an adverse effect on the separability of other classes such as vegetation, water bodies, and bare soil, and then leads to unsatisfactory classification accuracy. Users often aim at enhancing application relevant features in the fused product (Alparone, et al. 2004). An appropriate choice of a feature selection rule depends on the considered

* Corresponding author. Tel.: +84-043-838-7987.
E-mail address: caoxuancuongtd@gmail.com.

application (Chibani, 2007). Alparone et al., 2004 supposed the intensity modulation based fusion for the integrating of Panchromatic (PAN) and SAR textures into multispectral (MS) images. A threshold was used to control the amount of integration, which in turn improves slightly overall accuracy of classification.

Chibani proposed a hybrid fusion technique with wavelet transform to inject PAN and SAR features into MS images (Chibani, 2006 and 2007). The key idea of this method is that the integration of PAN and SAR images, as a new intensity component, and the original intensity component made a ratio which is used to locally modulate the MS images. In order to control the amount of SAR features to be injected into MS images, the author proposed some different selective fusion rules to integrate SAR and PAN images.

While the IHS method can be implemented to only three spectral bands at a time, the PCA can be utilized to merge more than three bands. In addition, redundant information due to the similar behaviour of land cover types in adjacent spectral bands can be organized in the way that all output bands are uncorrelated (Amolins et al., 2007).

This study presents an investigation of the hybrid fusion methods of wavelet with selective injection rules. A comparison between fused products in term of visualization and statistics is to find the best appropriate method for SAR and optical integration.

2. Data and methodology

2.1. Collection of satellite data

The multi-temporal, multisource and different resolution satellite images were used in this study located in Ha Tien town, Kien Giang province, Vietnam. Radar data included an ERS-2 band C, an ALOS PALSAR, and a Sentinel 1 scene of the study area were acquired for three years 1998, 2008 and 2016, respectively (Table 1 and Fig. 1). For optical data, Landsat 5 scenes recorded by the Thematic Mapper (TM) sensor and Landsat 8 OLI scene were collected for 1998, 2008 and 2016. These images were stored in GeoTIFF format, and featured in the UTM projection with WGS-84 datum.

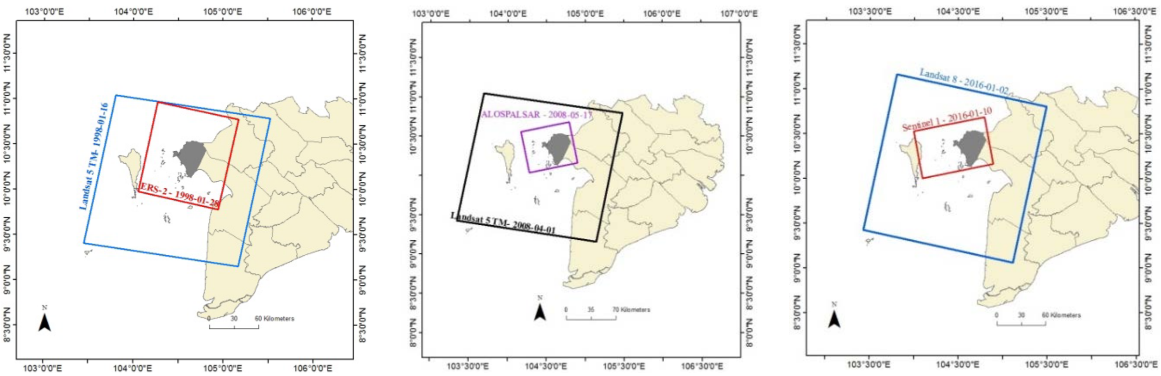

(a) (b) (c)

Fig. 1. The research area overlaid by the footprints of satellite data: (a) Year 1998; (b) Year 2008; (c) Year 2016

Table 1. Characteristics of images used in this study.

	1998		2008		2016	
	Landsat 5 TM	ERS-2	Landsat 5 TM	ALOSPALSAR	Landsat 8 OLI	Sentinel 1
Acquired Date	16th Jan	28th Jan	1st April	17th May	10th Jan	2nd Jan
Sensor	TM	ERS-2	TM	PALSAR/FBS	OLI	C-SAR
Spatial resolution	30 m	25 m	30 m	12 m	30 m	20
Flight direction		Descending		Ascending		Descending
Polarization		VV		HH		VV-VH
Swath	185 km	100 km	185 km	80 km	185 km	250 km
Incident angle	98.2°	23°	98.2°	41.5°		98.18°

2.2. IHS - Wavelet fusion method

The IHS and wavelet fusion method proposed by ((Nunez et al., 1999; Hong et al., 2009) is implemented to merge SAR and Landsat 5 TM imageries. However, instead of using decimated algorithm the ‘a trous’ algorithm is used to apply the wavelet transform action. The process is shown in Fig. 2:

Step 1: perform co-registration of both images, resample the Landsat 5 TM to get the spatial resolution equals to that of SAR image;

Step 2: apply IHS transform to Landsat 5 TM images to get intensity band, then perform histogram matching between the intensity and the SAR image;

Step 3: apply 'a trous' wavelet decomposition to both the intensity and histogram matched SAR imageries. As a result, from each the intensity or histogram matched SAR, one approximation plane (A) and three detail planes (D_i) are obtained;
Step 4: inject wavelet coefficients extracted from the SAR decomposition into the intensity band by a weighted combination model. This is to avoid an over injection of the intensity information; and
Step 5: perform inverse AWT and inverse IHS to achieve the fused images.
The weighted combination model can be expressed as:

$$A^{I+S} = w_1 . A^I + w_2 . A^S \quad (1)$$

where A^{I+S} is the new approximation band of the histogram-matched SAR. A^I and A^S are the approximation band of the intensity and the histogram-matched SAR, respectively, and w_1 and w_2 are the corresponding weight coefficients, which are expressed as follows:

$$w_1 = corr(\frac{A^I}{A^S}) \, , w_2 = 1 - w_1 \quad (2)$$

where $corr(\frac{A^I}{A^S})$ is the correlation coefficient between A^S and A^I.

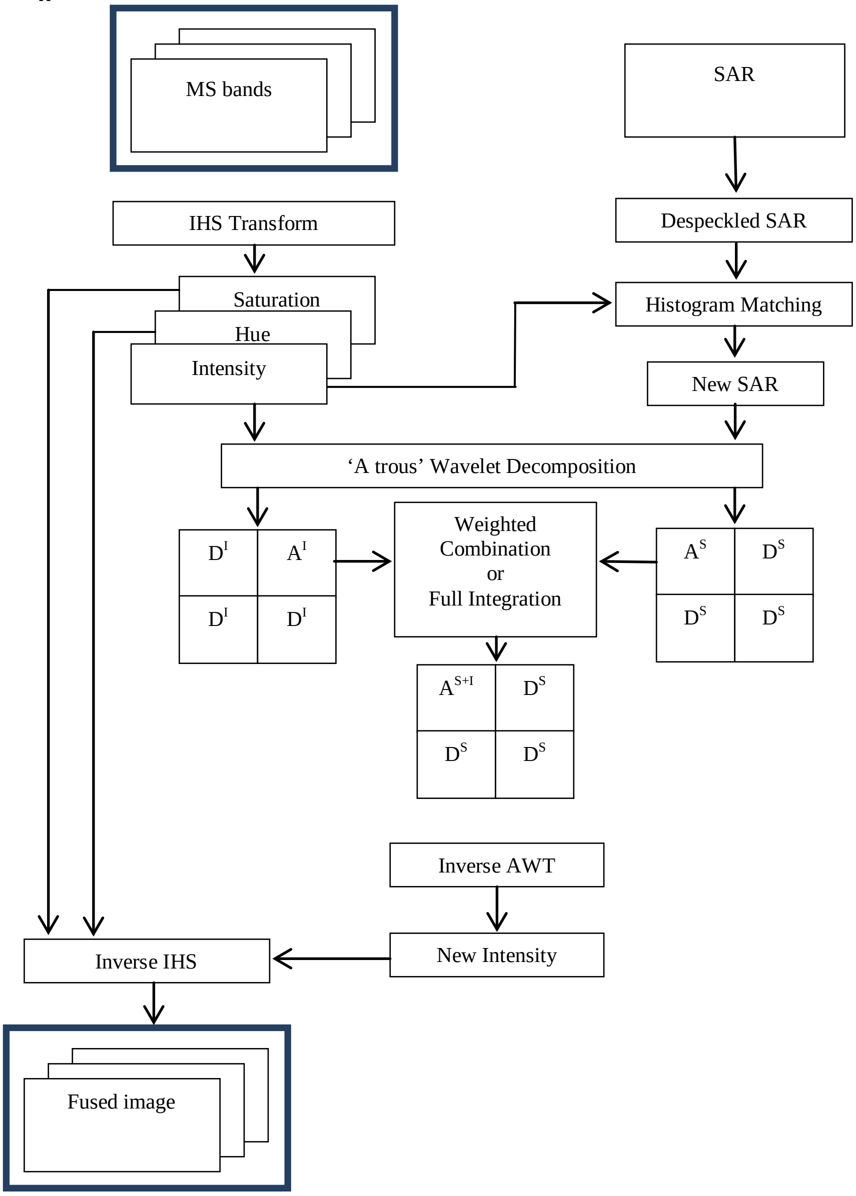

Fig. 2. IHS and Wavelet fusion method (modified after Hong et al., 2009).

2.3. PCA - Wavelet fusion method

The PCA and wavelet fusion scheme proposed by (Gonzalez-Audicana et al., 2004) is used in this study. The process is shown in Fig. 3. There are several steps to fuse SAR and Landsat 5 TM images:

Step 1: perform co-registration of both images, resample the Landsat 5 TM to get the spatial resolution equals to that of SAR image;
Step 2: apply PCA transform to Landsat 5 TM images to get PC1 image, and then perform histogram matching between PC1 and SAR images;
Step 3: apply 'a trous' wavelet decomposition to both the PC1 and histogram matched SAR imageries. As a result, from each the PC1 or histogram matched SAR, one approximation plane (A) and three detail planes (D_i) are obtained;
Step 4: inject wavelet coefficients extracted from the SAR decomposition into the PC1 band by a weighted combination model or a full integration model. The former is to avoid an over injection of the PC1 information, whereas the latter is to improve the separability of classes;
Step 5: perform inverse AWT and inverse PCA to achieve fused images.
The weighted combination model can be expressed as:

$$A^{PC1+S} = w_1.A^{PC1} + w_2.A^S \qquad (3)$$

where A^{PC1+S} is the new approximation band of the histogram-matched SAR, and A^{PC1} and A^S are the approximation band of the PC1 and the histogram-matched SAR, respectively, and w_1 and w_2 are the corresponding weight coefficients, which are expressed as follows:

$$w_1 = \frac{S_2^2}{S_1^2+S_2^2}, \quad w_2 = \frac{S_1^2}{S_1^2+S_2^2} \qquad (4)$$

where S_1, S_2 are standard deviation of A^{PC1} and A^S, respectively.

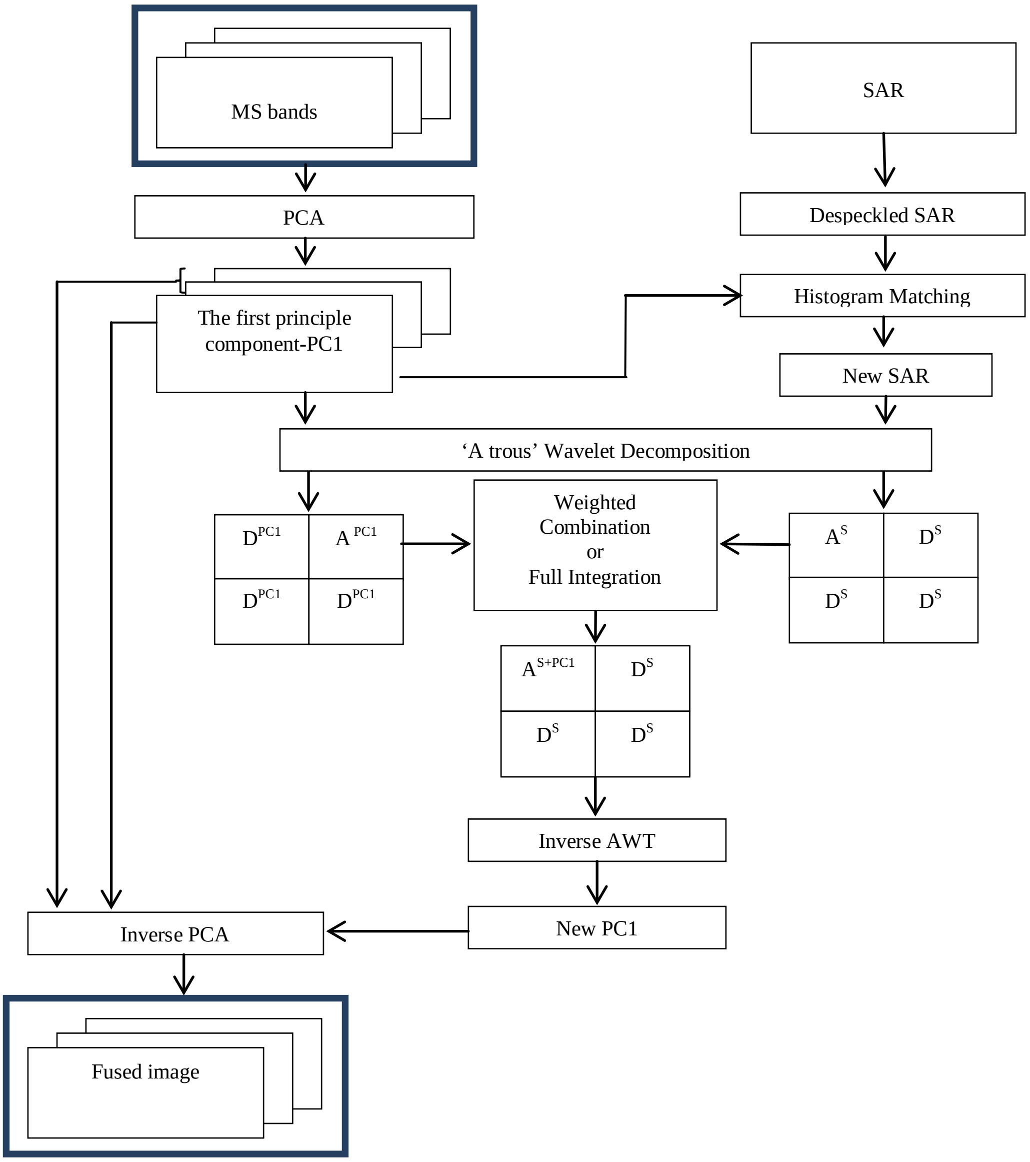

Fig. 3. PCA and Wavelet fusion method (modified after Hong et al., 2009).

2.4. Statistical evaluation of fusion performance

The evaluation of fusion performance is in both visual and quantitative (Alparone et al., 2007). Two of the most crucial criteria in fusion assessment are the spectral and spatial effects of the fused products. The closer the colour of the merged image is to that of the original multispectral image, the better the spectral effect of the merging method and the more details the merged image shows, the better the spatial effect of the merging method (Zhang, 1999).

Three statistical indices, namely Bias of mean (BM), correlation coefficient (CC) and standard deviation difference (SD), are used in the quantitative assessement of fusion performances (Amarsaikhan et al., 2012; Wald et al., 1997). The equations of these indices are expressed as follows:

- Bias of mean: $BM = \mu_{ori} - \mu_f$ (5)
- Correlation coefficient: $CC = \frac{\sum_i (I_i - \mu_{ori})(F_i - \mu_f)}{\sqrt{\sum_i (I_i - \mu_{ori})^2}\sqrt{\sum_i (F_i - \mu_f)^2}}$ (6)
- Standard deviation difference: $SD = \sigma_{ori} - \sigma_f$ (7)

where μ_{ori} and μ_f are the mean of original spectral image (I) and the fused image (F), respectively. σ_{ori} and σ_f are the standard deviation of original spectral image (I) and the fused image (F), respectively.

The ideal value of *BM* and *CC* are zero and one, respectively, while the lower value of *SD* is better. The *CC* value is closer to one, the fused image is less spectral distortion.

In order to estimate the amount of information injected into multispectral images, the entropy information (EI) is utilized. The formula of EI is expressed as:

$$EI = \sum_{n=0}^{255} P_n log P_n \quad (8)$$

where P_n is the histogram distribution of the image.

3. Results and discussion

3.1. Fused results of Landsat 5 TM and SAR imagery (ERS-2 and ALOSPALSAR)

In this study, two pairs of images, ERS-2 and Landsat 5 TM, and ALOSPALSAR and Landsat 5 TM, were merged using the two above-mentioned hybrid fusion methods. The Landsat 5 TM images are in 30 m spatial resolution, while the ERS-2 and ALOS PALSAR images are in 20 m and 12 m spatial resolution, respectively. Therefore, before image fusion, the MS images of Landsat TM were resampled to have the same spatial resolutions as the SAR images. The performance of the two fusion methods was evaluated using statistical indices to find the best one. The fused data of the best one was used for classifying the study area.

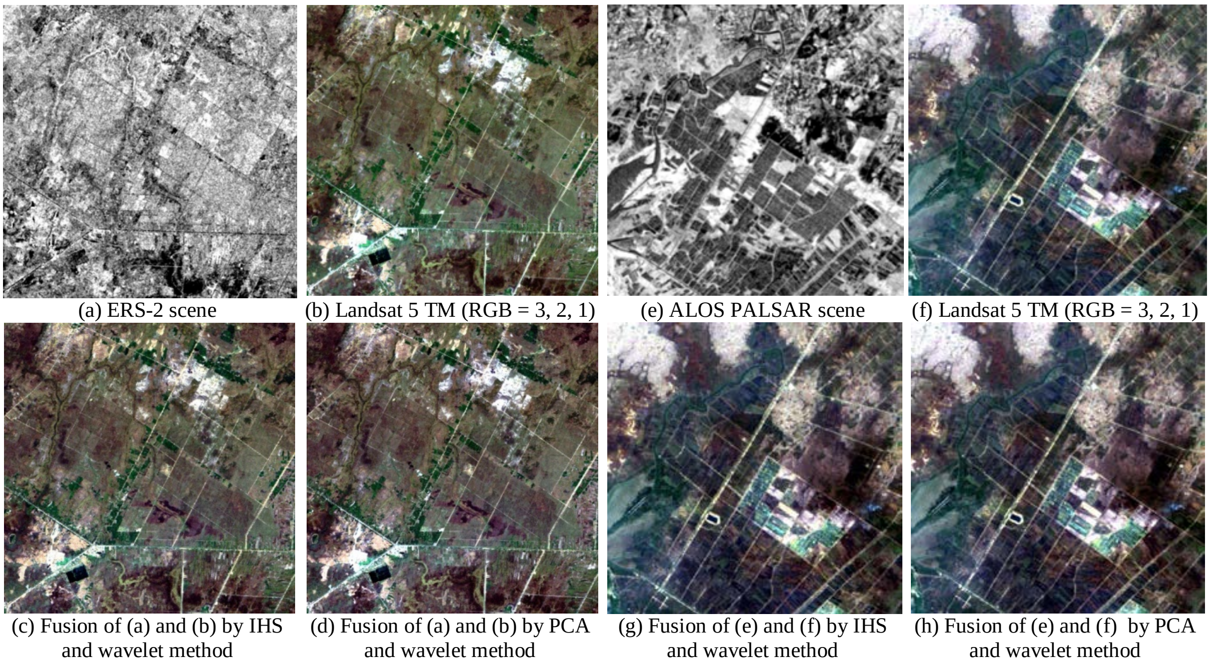

(a) ERS-2 scene (b) Landsat 5 TM (RGB = 3, 2, 1) (e) ALOS PALSAR scene (f) Landsat 5 TM (RGB = 3, 2, 1)

(c) Fusion of (a) and (b) by IHS and wavelet method (d) Fusion of (a) and (b) by PCA and wavelet method (g) Fusion of (e) and (f) by IHS and wavelet method (h) Fusion of (e) and (f) by PCA and wavelet method

Fig. 4. (a,b,c,d) Fused results of ERS-2 and Landsat 5 TM data; (e,f,g,h) Fused results of ALOS PALSAR and Landsat 5 TM data

While it might be simple to assess the quality of fused results by visual inspection, the statistical comparison can assess quantitatively the performance of each image fusion method (Chibani, 2006). It can be observed from Table 4 that all the ERS-2 and Landsat TM images fused using the two methods have high CC values. This underpins the obvious similarity in the appearance of the fused results and original MS images. However, after fusing the detail of ERS-2 image into MS images using the PCA-wavelet method, the CC between the fused products and the original MS images are higher than those fused by using the IHS-wavelet method in almost all bands. ERS2-Band 1 and ERS2-Band 2 images fused using the PCA-wavelet method have much higher CC values than those fused by the IHS-wavelet method, whereas only the CC value from ERS2-Band 5 image fused by the latter method is slightly larger than that by the former method. In terms of BM and SDD values, almost all the BM and SDD of images fused using the PCA-wavelet method are lower than those fused using the IHS-wavelet method. A similar figure is seen in the case of ALOS PALSAR and Landsat TM fusion (Table 2).

Table 2. Statistical evaluation of ERS-2 and Landsat 5 TM fusion and of ALOS PALSAR and Landsat 5 TM fusion

	Fusion of Landsat 5 TM and ERS-2						Fusion of Landsat 5 TM and ALOS PALSAR					
	IHS and wavelet			PCA and wavelet			IHS and wavelet			PCA and wavelet		
Band	CC	BM (10^-4)	SDD (10^-4)	CC	BM (10^-4)	SDD (10^-4)	CC	BM (10^-4)	SDD (10^-4)	CC	BM (10^-4)	SDD (10^-4)
Ideal	**1**	**0**	**0**	**1**	**0**	**0**	**1**	**0**	**0**	**1**	**0**	**0**
1	0.7917	4.4	7.5	0.9681	1.6	0.4	0.8947	2.8	4.4	0.9935	0.6	0.1
2	0.8981	4.1	0.3	0.9604	2.3	0.6	0.9628	2.6	0.6	0.9925	1	0.3
3	0.9445	4.4	4.6	0.9556	3.3	0.9	0.9850	2.6	1.9	0.9889	1.8	0.6
4	0.9204	8	8.5	0.9772	5.3	0.3	0.9457	6.6	13	0.9855	5.0	0.2
5	0.9315	10	0.7	0.9216	10	0.3	0.9855	10	1.4	0.9797	11	0.6
6	0.9536	6.2	3.4	0.9291	7.4	0.1	0.9878	6.6	2.8	0.9803	7.9	0.2

3.2. Fused results of Landsat 8 OLI and Sentinel-1 SAR

The spatial resolutions of Landsat 8 MS, PAN, and Sentinel-1 images were 30, 15, and 20 m respectively. Therefore, before image fusion, the Sentinel-1 and MS images were resampled to the same spatial resolution as the Landsat 8 PAN image. Fig. 5a and 5b shows the result of integrating Landsat 8 PAN and Sentinel-1 images using two models, namely full integration (FI) model and weighted combination (WC) model. The two PAN-Sentinel-1 scenes fused by the two models were used to fuse with MS images using the PCA-wavelet fusion method (Fig. 5d and 5e). Generally, it can be seen from Table 3 that all fused images have high CC values. Furthermore, the CC between the images fused by using the full combination mode and original MS images is slightly lower than those by the weighted combination model. When comparing the CC and BM values among fused bands, fused bands 1, 2, and 3 have CC values higher than fused bands 4, 5, and 6, whereas the first three fused bands have BM values much lower than the last three. These larger distortions in spectral values of the fused bands 4, 5, and 6 are caused by the difference in the wavelength of the PAN image and the last three bands. The smaller spectral distortion of the fused images by the weighted combination model compared to that by the full integration model is due to the former model injecting fewer details from the SAR image into the MS image than the latter does. As the amount of information contained in an image is normally measured by entropy information (Chibani & Houacine, 2003), entropy values from Table 4 underpin this point as the larger the entropy value is the more information from the SAR image introduced in MS images. Moreover, the difference in the wavelength of SAR data and MS data creates the spectral distortion of fused data.

a. PAN-Sentinel-1 fused scene by full integration model

b. PAN-Sentinel-1 fused scene by weighted integration model

c. Landsat 8 (RGB = band 4, 3, and 2)

d. By full integration model

e. By weighted integration model

Fig. 5. Fusion results of Sentinel-1 and Landsat 8 using FI model, WC model with PCA-wavelet fusion method

Table 3. Statistical evaluation results of Sentinel-1 and Landsat 8 fusion

Band	Full Integration (FI) model			Weighted Combination (WC) model		
	CC	BM (10^-4)	SDD (10^-4)	CC	BM (10^-4)	SDD (10^-4)
Ideal	**1**	**0**	**0**	**1**	**0**	**0**
1	0.9976	0.2	0.08	0.9980	0.2	0.2
2	0.9828	0.7	0.5	0.9856	0.6	0.9
3	0.9962	0.5	0.2	0.9968	4.6	0.6
4	0.8999	13	0.6	0.9158	12	1.5
5	0.9137	7.8	0.5	0.9276	7.2	1.5
6	0.9379	3.8	0.2	0.9480	3.5	1.7

Table 4. Entropy information of images

Band	Entropy Information		
	Original	WC	FI
1	2.9024	2.9186	2.9219
2	3.5729	3.5750	3.5757
3	4.1123	4.1344	4.1396
4	6.6230	6.6672	6.6717
5	6.0129	6.0484	6.0483
6	5.1276	5.1531	5.1532

Since the spectral distortion of the images fused by the full integration model is small and the images obtain more information from Sentinel-1, for the purpose of classification, full integration was the best model as it might help to improve the separability of classes (Chibani, 2007).

3.3. Discussion

The comparison between two wavelet-based fusion schemes, IHS and wavelet, and PCA and wavelet, demonstrated that the PCA-wavelet method performed better than the IHS-wavelet when they were applied to integrate Landsat data and SAR data. Furthermore, two models of injecting spatial information extracted from SAR data into MS images, namely full integration and weighted combination models, were utilized in the fusion procedure. Experimental results illustrated that the two fusion methods with both injection models performed well with fast processing time and low complexity. However, spectral distortion occurred in all cases. Colour distortion was introduced into the resulting products because of significant differences in gray values between SAR and MS images. This inevitable issue is due to different characteristics of sensors. The efficiency of colour preservation depends on the amount of fusion data. As the relationship between the spectral and spatial resolutions is inverse (El-Mezouar et al., 2011), the more spatial information to be fused, the more spectral distortion occurs. It is noted that PCA is a data reduction technique. Although the IHS smoothly integrated the spatial resolution information, it could not reduce the amount of redundancy in information of adjacent MS bands. In addition, a comparison between the two models of injection revealed that the fused images produced by the full combination model were more distorted in spectral value than those produced by the weighted integration model. This could be due to the former injecting more spatial information extracted from SAR data into fused products than the latter. However, the spectral distortion in fused products obtained by using both models was satisfactory. In addition, the full combination model performed maximal integration of SAR features. It is noted that the full integration model is to improve class distinctiveness. Therefore, this model was chosen to integrate SAR and MS images in this research.

4. Conclusion

The study has performed the integration of three pairs of multi-source images including Landsat 5 TM and ERS-2, Landsat 5 TM and ALOS PALSAR, and Landsat 8 OLI and Sentinel-1 data. Two hybrid fusion methods of wavelet were used, namely IHS-wavelet and PCA-wavelet. The study revealed that PCA-wavelet is better than IHS-wavelet in reducing spectral distortion. When spatial details derived from SAR data were injected into MS images, weighted combination and full integration models were employed. Images fused by the weighted combination model were less distorted in spectrum than those by the full integration model but they contained less spatial information. While both models preserved spectral values, the full integration model was the best choice for the model of injection in PCA-wavelet method for the purpose of separability of classes.

Acknowledgements

The ERS-2 SAR data were provided by the European Space Agency to N. V. Trung as a Category-1 project (PI No. 19170). The ALOS PALSAR data were provided by JAXA and Landsat data were provided by NASA.

References

Alparone, L., Baronti, S., Garzelli, A., & Nencini, F. (2004). Landsat ETM+ and SAR image fusion based on generalized intensity Modulation. *Geoscience and Remote Sensing, IEEE Transactions on, 42*(12), 2832-2839. doi:10.1109/TGRS.2004.838344

Alparone, L., Wald, L., Chanussot, J., Thomas, C., Gamba, P., & Bruce, L. M. (2007). Comparison of Pansharpening Algorithms: Outcome of the 2006 GRS-S Data-Fusion Contest. *IEEE Transactions on Geoscience and Remote Sensing, 45*(10), 3012-3021. doi:10.1109/TGRS.2007.904923

Amarsaikhan, D., Saandar, M., Ganzorig, M., Blotevogel, H. H., Egshiglen, E., Gantuyal, R., . . . Enkhjargal, D. (2012). Comparison of multisource image fusion methods and land cover classification. *International Journal of Remote Sensing, 33*(8), 2532-2550. doi:10.1080/01431161.2011.616552

Amolins, K., Zhang, Y., & Dare, P. (2007). Wavelet based image fusion techniques — An introduction, review and comparison. *ISPRS Journal of Photogrammetry and Remote Sensing, 62*(4), 249-263. doi:http://dx.doi.org/10.1016/j.isprsjprs.2007.05.009

Byun, Y., Choi, J., & Han, Y. (2013). An Area-Based Image Fusion Scheme for the Integration of SAR and Optical Satellite Imagery. *Selected Topics in Applied Earth Observations and Remote Sensing, IEEE Journal of, 6*(5), 2212-2220. doi:10.1109/JSTARS.2013.2272773

Chibani, Y. (2006). Additive integration of SAR features into multispectral SPOT images by means of the à trous wavelet decomposition. *ISPRS Journal of Photogrammetry and Remote Sensing, 60*(5), 306-314. doi:http://dx.doi.org/10.1016/j.isprsjprs.2006.05.001

Chibani, Y. (2007). Integration of panchromatic and SAR features into multispectral SPOT images using the 'à trous' wavelet decomposition. *International Journal of Remote Sensing, 28*(10), 2295-2307. doi:10.1080/01431160600606874

Chibani, Y., & Houacine, A. (2003). Redundant versus orthogonal wavelet decomposition for multisensor image fusion. *Pattern Recognition, 36*(4), 879-887. doi:http://dx.doi.org/10.1016/S0031-3203(02)00103-6

El-Mezouar, M. C., Taleb, N., Kpalma, K., & Ronsin, J. (2011). An IHS-Based Fusion for Color Distortion Reduction and Vegetation Enhancement in IKONOS Imagery. *IEEE Transactions on Geoscience and Remote Sensing, 49*(5), 1590-1602. doi:10.1109/TGRS.2010.2087029

Gonzalez-Audicana, M., Saleta, J. L., Catalan, R. G., & Garcia, R. (2004). Fusion of multispectral and panchromatic images using improved IHS and PCA mergers based on wavelet decomposition. *IEEE Transactions on Geoscience and Remote Sensing, 42*(6), 1291-1299. doi:10.1109/TGRS.2004.825593

Hong, G., Zhang, Y., & Mercer, B. (2009). A Wavelet and IHS Integration Method to Fuse High Resolution SAR with Moderate Resolution Multispectral Images. *Photogrammetric Engineering & Remote Sensing, 75*(10), 1213-1223. doi:10.14358/PERS.75.10.1213

Nunez, J., Otazu, X., Fors, O., Prades, A., Pala, V., & Arbiol, R. (1999). Multiresolution-based image fusion with additive wavelet decomposition. *IEEE Transactions on Geoscience and Remote Sensing, 37*(3), 1204-1211. doi:10.1109/36.763274

Pohl, C., & Van Genderen, J. L. (1998). cReview article Multisensor image fusion in remote sensing: Concepts, methods and applications. *International Journal of Remote Sensing, 19*(5), 823-854. doi:10.1080/014311698215748

Wald, L., Ranchin, T., & Mangolini, M. (1997). Fusion of satellite images of different spatial resolutions: Assessing the quality of resulting images. *Photogrammetric Engineering and Remote Sensing, 63(6)*, 691-699.

Zhang, Y. (1999). A new merging method and its spectral and spatial effects. *International Journal of Remote Sensing, 20*(10), 2003-2014. doi:10.1080/014311699212317